Impact of a molecular wetting layer on the structural and optical properties of tin(II)-phthalocyanine multilayers on Ag(111)

Marco Gruenewald, Julia Peuker, Matthias Meissner, Falko Sojka, Roman Forker, and Torsten Fritz*
Friedrich-Schiller-Universität Jena, Institut für Festkörperphysik, Helmholtzweg 5, 07743 Jena, Germany
(Received 8 December 2015; published 11 March 2016)

We investigate ultrathin highly ordered layers of tin(II)-phthalocyanine (SnPc) on top of a monolayer (ML) of 3,4,9,10-perylenetetracarboxylic dianhydride (PTCDA) on Ag(111). The films are analyzed structurally by means of scanning tunneling microscopy (STM) and low-energy electron diffraction (LEED) as well as optically using differential reflectance spectroscopy (DRS). We find that the first ML of SnPc is entirely rearranged upon bilayer (BL) formation, yielding a commensurate registry in higher-order coincidence with the underlying PTCDA lattice. SnPc layers adsorbed on top self-assemble in further BLs. Within each BL the molecules are arranged pairwise, i.e., stacked as physical dimers, providing a characteristic absorption spectrum with strongly redshifted components compared to SnPc monomers. This altered spectral envelope mainly originates from strong orbital overlap of stacked molecules within each BL. In contrast, adjacent BLs show only weak orbital overlap, which is responsible for an additional redshift of the low-energy transition band. Our results demonstrate that a simple modification of the metal substrate surface, e.g., by a PTCDA wetting layer, has beneficial effects on structural ordering of SnPc multilayers adsorbed on top. The impact on the optical absorption spectrum manifests in a narrow and intense absorption peak in the near-infrared spectral region which is significantly less pronounced if the PTCDA layer is omitted.

DOI: 10.1103/PhysRevB.93.115418

I. INTRODUCTION

In recent years organic thin films have attracted much interest owing to their beneficial properties in field effect transistors (OFET), organic light-emitting diodes (OLED), and organic photovoltaic devices (OPVD) [1–3]. Typically, such devices consist of several thin layers, each providing a specific functionality (e.g., charge-carrier injection, transport, or blocking) [2,4]. If low trap or defect densities are of paramount importance, designing the respective layers as highly ordered films can further improve the overall performance of the device [5]. It is expected that such layers will also play an important role in future applications like organic lasers and logical devices [6,7]. A broader applicability of such layers, however, is still hampered by challenging preparation conditions. Organic molecular beam epitaxy (OMBE) can be used for the growth of such films and corresponding interfaces. While OMBE is, in general, capable of producing highly ordered layers with low defect densities, a variety of parameters (e.g., molecule-substrate and molecule-molecule interactions, molecular symmetries, temperature-dependent surface mobility) has substantial influence on the structures and morphologies formed. In particular, the substrate used can strongly alter the characteristics of the adsorbate film. Even a simple modification of the substrate surface, e.g., by an intermediate organic wetting layer, can have beneficial or disadvantageous effects on the further film growth and the charge-transport characteristics [4,8,9].

Here we focus on epitaxially grown model systems consisting of tin(II)-phthalocyanine (SnPc) and 3,4,9,10-perylenetetracarboxylic dianhydride (PTCDA) layers on Ag(111). While PTCDA is planar in the gas phase, SnPc is shuttlecock shaped owing to the presence of the relatively large Sn atom protruding from the tetraazaporphine ring. SnPc can thus adsorb on surfaces in different configurations (Sn-up and Sn-down). In this context SnPc is a representative of the group of shuttlecock-type phthalocyanines. For example, lead(II)-phthalocyanine (PbPc) and titanyl phthalocyanine (TiOPc) are known to form comparable structures and behave similarly in terms of their optical absorption [10–13].

It shall be elucidated here that the film quality of SnPc multilayers can be strongly enhanced simply by adding an ultrathin PTCDA interlayer. For structural clarification we use low-energy electron diffraction (LEED) and low-temperature scanning tunneling microscopy (STM). The effects of the additional organic heterointerface in terms of electronic coupling (orbital overlap) and coupling of transition dipole moments of SnPc are discussed on the basis of *in situ* differential reflectance spectroscopy (DRS) measurements.

The optical properties of metal phthalocyanines in the gas phase, in solution, and in aggregated form have been studied experimentally as well as theoretically [11,14,15]. For isolated molecules a narrow monomer absorption band (Q band) can be observed in the visible spectral region (VIS) [14,15]. When the molecules form aggregates, the spectral fingerprint can be altered significantly, e.g., by transition dipole coupling [16]. The notations H and J aggregates are commonly used to describe the two extreme cases where the transition dipole moments are side by side and head to tail, respectively [17]. The latter case is responsible for a spectral redshift of the transition energies of the aggregate compared to the monomer, making the near-infrared (NIR) spectral region available for light absorption and emission [17,18].

The starting point of our investigations is a monolayer (ML) of SnPc on 1 ML PTCDA/ Ag(111) which has been thoroughly investigated optically and structurally in a previous publication [19]. Briefly, it was found that SnPc forms either a gaslike phase or large highly ordered domains exhibiting several different commensurate registries with relatively large unit

*torsten.fritz@uni-jena.de

cells as a function of coverage. In this contribution we show that the SnPc monolayer in contact with the PTCDA wetting layer is entirely rearranged upon formation of the SnPc bilayer (BL), which itself exhibits a type-II coincidence with the PTCDA lattice (as defined by Hooks *et al.*, also referred to as higher order commensurate [20,21]). Further SnPc adsorbates also arrange themselves as BLs in a comparable structure. DRS data indicate that the orbital overlap between the molecules within the BLs is much stronger than between adjacent BLs. The stacked SnPc aggregates primarily exhibit J-type character with a narrow absorption peak in the NIR which, by comparison with previous work [22], differs noticeably if the PTCDA interlayer is omitted.

II. EXPERIMENTAL DETAILS

The thin films were deposited from effusion cells under ultrahigh-vacuum conditions (base pressure 10^{-10} mbar) at room temperature (RT) onto the Ag(111) substrate initially cleaned by repeated Ar^+-sputtering and annealing cycles [23]. The PTCDA monolayer was prepared by depositing multilayers followed by annealing at 600 K [24–26]. SnPc was deposited on top with a growth rate of approximately 0.1 ML per minute monitored by *in situ* DRS.

The structures were analyzed by means of STM (SPECS JT-LT-STM/AFM with KolibriSensors^{TM}) operating at $T = 1.1$ K [27]. To analyze epitaxy relations in reciprocal space a combination of LEED measurements [dual microchannel plate (MCP) LEED from OCI Vacuum Microengineering] and fast Fourier transformed (FFT) STM images were used. For LEED measurements the samples were cooled from RT to ≈ 20 K. No structural reorganization could be detected upon cooling. The LEED images have been numerically corrected for geometric distortion and for the primary electron energy offset prior to the analysis [28,29].

Detailed information about our DRS setup can be found elsewhere [30,31]. Briefly, it represents a variant of *in situ* absorption spectroscopy using a light beam at a 20° incident angle with respect to the sample surface. For this a 100 W halogen lamp is used, operated with a stabilized power supply (Müller Elektronik-Optik). The reflected light is then spectrally analyzed by means of a monochromator (Acton Research SpectraPro SP2356) where a charge-coupled device (CCD) is attached (Princeton Instruments Spec-10 100BR, liquid nitrogen cooled). DRS measures the relative change of reflectance during the film deposition according to $\mathrm{DRS}(E,d) := [R(E,d) - R(E,0)]/[R(E,0)]$, where $R(E,d)$ is the reflectance of the sample surface covered with a film of thickness d. Consequently, the DRS signal depends not only on the optical constants of the adsorbate but also on the substrate used. We thus extracted the complex dielectric function $\varepsilon(E,d) = \varepsilon'(E,d) - i\varepsilon''(E,d)$ of the adsorbate films by a numerical algorithm where multiple reflections and interference effects were taken into account. For this purpose the thicknesses of a monolayer of PTCDA ($d_{\mathrm{PTCDA}} = 0.32$ nm [32,33]) and SnPc ($d_{\mathrm{SnPc}} = 0.34$ nm [34,35]) were used by the algorithm. Since the real and imaginary parts of the dielectric function ε' and ε'' are connected by a Kramers-Kronig relation, we will restrict our discussion to the imaginary part. For the molecules investigated here it is known that the condensation into a densely packed monolayer with flat-lying molecules has only a marginal effect on the optical spectra, whereas the spectral envelope changes markedly upon three-dimensional aggregation (stacking) [22]. Consequently, deposition rates and thus film thicknesses were calibrated by means of these distinct transitions in the optical spectra occurring when a new monolayer starts to grow. The first ML of SnPc on 1 ML PTCDA/Ag(111) is filled completely prior to the growth of multilayers, which was checked by means of STM.

Optical absorbance spectra of SnPc dissolved in benzene were recorded at room temperature with an *ex situ* UV-VIS spectrophotometer Cary 5000 from Varian.

III. RESULTS AND DISCUSSION

A. Structural characterization

In order to investigate the bilayer structure we start with a 1.5 ML SnPc adlayer on 1 ML PTCDA/Ag(111). Such films mainly consist of densely packed domains and some individual molecules loosely distributed in the second ML of SnPc. The first SnPc ML thus intentionally remains partially uncovered.

The SnPc ML structure on top of PTCDA/Ag(111), depicted in Fig. 1(a), is characterized by six SnPc molecules in the unit cell where four are in the Sn-up configuration and two are in the Sn-down configuration (see unit-cell sketch in the upper right corner), as previously reported in Ref. [19]. It can be seen that for very dilute regions of the second ML single molecules (highlighted by white dashed circles) adsorb in a stacked geometry, supposedly maximizing the intermolecular $\pi-\pi$-orbital overlap. The single second-layer molecules thereby have no significant influence on the lateral structure of the underlying SnPc. Such a stacking is thought to be typical for phthalocyanine dimers in solution [18].

The STM image in Fig. 1(b) shows a highly ordered structure of the second ML of SnPc, which can be described by a unit cell (parameters compiled in Table I) exhibiting one Sn-down molecule in the second SnPc layer. We find that in our case large domains (up to several 100 nm in diameter) with a very low defect concentration are formed. The domain size is thereby affected by molecular defects of the first ML of SnPc predominantly located at silver steps (see Fig. 1 in the Supplemental Material [36]). Those appear to act as diffusion barriers for SnPc molecules in the second layer, as can be inferred from Fig. 1(b).

Furthermore, we frequently find that the first SnPc ML exhibits a high density of molecular defects near a domain boundary of the second SnPc ML, obviously not caused by silver steps, as can be seen in Fig. 1(c). A possible explanation could be provided by one of the following scenarios: (i) a PTCDA domain boundary induces the defects of the first SnPc ML, and consequently, the growth of the second SnPc ML is hampered locally, or (ii) the second SnPc ML induces the alteration of the first SnPc ML. As evidenced from the FFTs of the lower left and upper right corners of Fig. 1(c) (not shown), we find that if there were different PTCDA domains lying underneath, they would definitely have the same orientation toward the substrate. Thus, dislocations of PTCDA could be the origin of the change in the SnPc arrangement. On the other hand, even in large scans ($\approx 100 \times 100\,\mathrm{nm}^2$) of a 1 ML

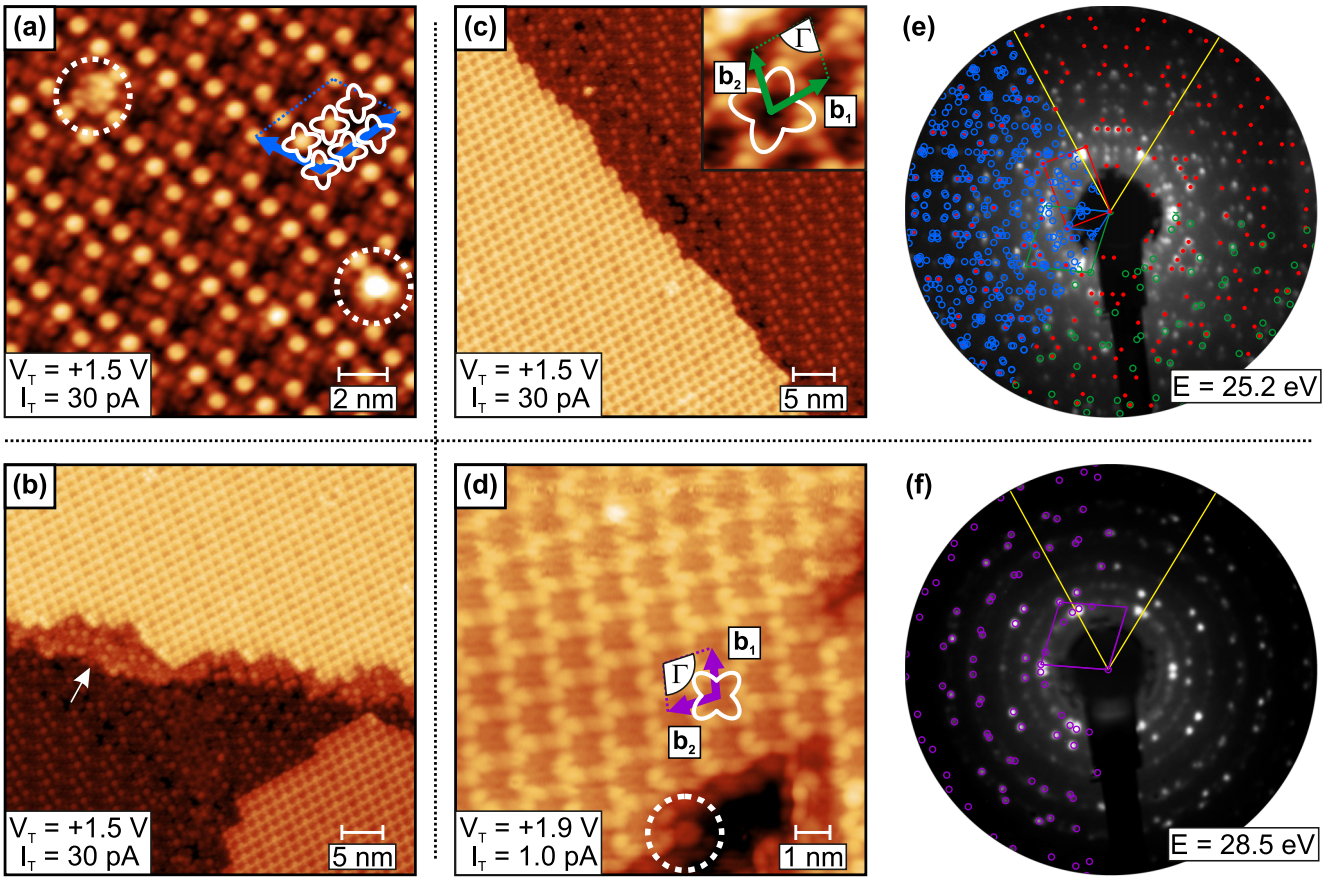

FIG. 1. STM images of a sample with a nominal SnPc coverage of (a)–(c) 1.5 ML and (d) 4 ML SnPc. In (a) individual molecules in the second ML of SnPc (highlighted by white dotted circles) are shown. The white arrow in (b) points at a substrate step edge. The surface unit-cell vectors of the SnPc BL with the one-molecule basis of the upper SnPc layer are shown as an inset in (c). (e) and (f) LEED patterns corresponding to the 1.5 and 4 ML films, respectively. LEED simulations of the SnPc BL (open green circles), the SnPc ML (open blue circles), and the 1 ML PTCDA/Ag(111) substrate (red dots) are superimposed on selected segments of the image in (e). A simulation of the 4 ML structure (open purple circles) is shown in (f). All films were grown on top of a 1 ML PTCDA/Ag(111) substrate whose LEED pattern remained unaffected by the SnPc adsorption. Two primitive directions of Ag(111) are indicated by yellow lines as a reference.

SnPc/1 ML PTCDA/Ag(111) sample, defects were found only very sporadically. Consequently, scenario (ii) seems to be far more likely.

In order to corroborate this interpretation, we extracted structural data of the stacked layers from LEED measurements [Figs. 1(e) and 1(f)]. The results are summarized in Table I. Further, an STM image of the SnPc BL on 1 ML PTCDA/Ag(111) is shown in Fig. 2(a). By calculating the corresponding FFT as shown in Fig. 2(b) reciprocal lattices can basically be analyzed in analogy to LEED. The FFT image consists not only of contributions from the surface unit cell of the SnPc BL (green dots) but also of frequencies stemming from the underlying PTCDA lattice (marked by red unit cell). Additional features arise from a long-range modulation of the SnPc lattice caused by the periodic potential of the PTCDA lattice. The arrangement of all spots in the FFT image can thus be simulated by a mere convolution of the lattices of SnPc and PTCDA (red dots) [37]. We point out that no contributions

TABLE I. Structural parameters of SnPc on 1 ML PTCDA/Ag(111). $\mathbf{b}_1$, $\mathbf{b}_2$: SnPc lattice vectors; Γ: unit-cell angle between $\mathbf{b}_1$ and $\mathbf{b}_2$; θ: SnPc domain angle between $\mathbf{b}_1$ and the PTCDA lattice vector $\mathbf{a}_1$. The epitaxy matrix of the SnPc bilayer is given with respect to the PTCDA lattice, which itself is described by $\mathcal{C}_{\mathrm{PTCDA}} = \begin{pmatrix} 3 & 5 \\ -6 & 1 \end{pmatrix}$ relative to the Ag(111) surface. The uncertainties of each matrix element refer to the standard deviation of the fitting routine. The primitive silver lattice vectors enclose an angle of 120°. Numbers in parentheses indicate the uncertainty of the last significant digit(s).

Structure	$\lvert\mathbf{b}_1\rvert$ (Å)	$\lvert\mathbf{b}_2\rvert$ (Å)	Γ (deg)	θ (deg)	Epitaxy matrix $\mathcal{C}$
SnPc bilayer	13.99(4)	13.59(4)	77.5(2)	−26.8(2)	$\begin{pmatrix} 1.001(2) & -0.333(1) \\ 0.668(3) & 0.556(2) \end{pmatrix}$
4 ML SnPc	13.9(4)	13.4(4)	77.6(2)		
(1 0 $\bar{1}$) plane of triclinic SnPc [35]	14.205(10)	12.630(3)	75.40(8)		

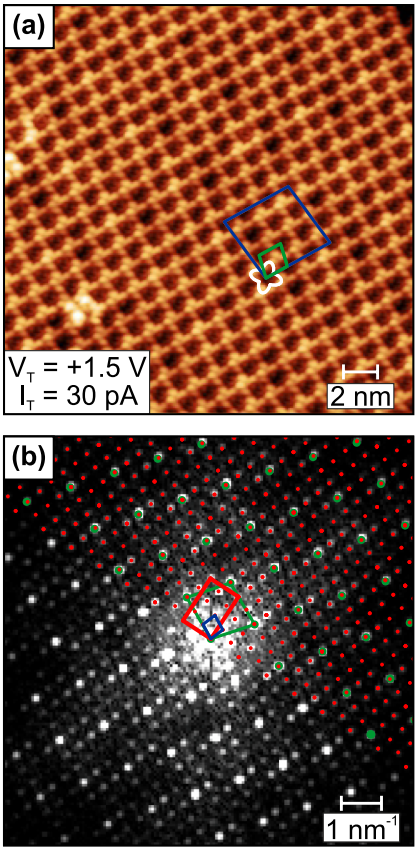

FIG. 2. (a) Zoom of the STM image of the SnPc bilayer shown in the lower left corner of Fig. 1(c). The primitive unit cell of the SnPc bilayer (green) as well as the commensurate supercell (dark blue) are superimposed. (b) Corresponding FFT with a plot of the reciprocal unit cells of PTCDA (red) and SnPc (green) determined by the lattice fit routine of LEEDLAB, and the convolution of both lattices (red dots). The commensurate reciprocal supercell is also superimposed (dark blue).

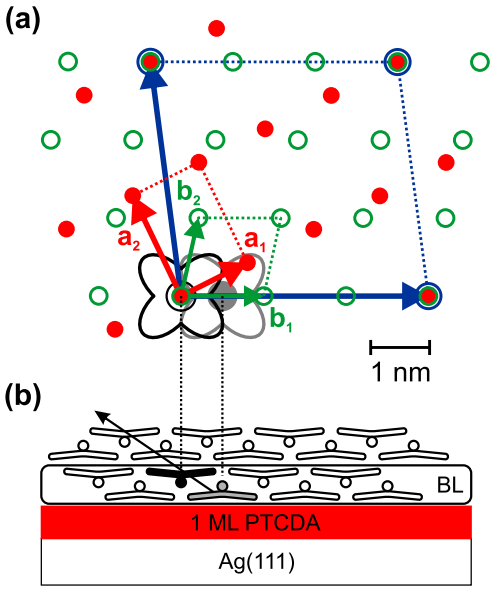

FIG. 3. (a) Real-space plot of the primitive SnPc BL lattice (open green circles) on 1 ML PTCDA/Ag(111) (red dots). The commensurate supercell is depicted in dark blue. Additionally, the proposed basis belonging to the primitive SnPc BL unit cell is shown, where a Sn-up (gray) and a Sn-down (black) molecule are located in the first and second SnPc layers, respectively. (b) Schematic side view of the proposed stacking of the SnPc layers. The first BL is indicated by the rounded box. The arrow points in stacking direction of the quasi-one-dimensional aggregates.

from the SnPc ML structure on 1 ML PTCDA/Ag(111) can be found in Fig. 2(b). From these findings we conclude that the first SnPc ML is entirely rearranged upon adsorption of the second SnPc ML, yielding the distinct BL structure. Hence, the characteristic motif of Sn-up and Sn-down arrangement of the first SnPc ML is not adopted by the second SnPc ML. Note that the ML phase and the BL phase of SnPc are simultaneously observed in Fig. 1(e) because LEED probes a macroscopic area of the sample where both phases coexist for the 1.5 ML SnPc film.

The epitaxy relation between SnPc and PTCDA has been determined by means of LEED and has been refined by analyzing the FFT image in Fig. 2(b) using LEEDLAB [28,29]. The real-space lattices of the PTCDA ML and the SnPc BL are illustrated in Fig. 3(a). The primitive SnPc lattice can be described by an epitaxy matrix $\mathcal{C}^{\text{primitive}}_{\text{SnPc}} = \begin{pmatrix} 1 & -1/3 \\ 2/3 & 5/9 \end{pmatrix}$, indicating a type-II coincidence [20] with respect to the PTCDA ML. It can be seen that the $[\bar{1}\,3]$ and $[3\,0]$ lattice vectors of SnPc coincide with the $[2\,1]$ and $[3\,\bar{1}]$ vectors of PTCDA; that is, a supercell (SC) of SnPc is commensurate to the PTCDA lattice in higher order [20,21]. By strongly contrast enhancing the STM image in Fig. 2(a) the SC can also be identified in real space (see Fig. 2 in the Supplemental Material). The epitaxy matrix of the SC has been determined to $\mathcal{C}^{\text{SC}}_{\text{SnPc}} = \begin{pmatrix} 3 & -1 \\ 1 & 2 \end{pmatrix}$. All epitaxy matrices are given with respect to the PTCDA lattice. The results are also in full agreement with the LEED measurement in Fig. 1(e).

Structural reorganizations as observed for the BL formation can have a significant influence on the orbital overlap of adjacent molecules and thus on the optical absorption behavior. The exact arrangement of the molecules within the unit cell is therefore of particular interest. While the upper layer of the densely packed SnPc BL obviously consists of only Sn-down molecules [see Figs. 1(b) and 1(c)], the configuration of the molecules in contact with PTCDA cannot be readily determined from STM images. The structural arrangement shall therefore be deduced from a comparison with the triclinic SnPc bulk structure available from Refs. [34,35]. The surface unit cell of the BL film is quite similar to the two-dimensional unit cell of the $(1\,0\,\bar{1})$ lattice plane of the SnPc triclinic structure (see Table I). Within this lattice plane the molecules are stacked pairwise in a slipped cofacial geometry, and the shuttlecock shapes of adjacent molecules in these pairs point at each other. The tilt angle of the molecular plane with respect to the $(1\,0\,\bar{1})$ lattice plane is $\approx 20^\circ$, giving rise to a significant length difference (1.6 Å) of the two unit-cell vectors. By contrast, in the BL structure observed here that difference between $|\mathbf{b}_1|$ and $|\mathbf{b}_2|$ is only 0.4 Å. We therefore expect that the molecules are tilted to a lesser extent, and they may even adsorb parallel to the surface. The suggested basis for the primitive unit cell of the SnPc BL is superimposed on the lattice plot in Fig. 3(a). The SnPc stacking in extended BL domains

thereby differs significantly from the face-to-face arrangement observed for single second-layer SnPc molecules with respect to the first SnPc ML, depicted in Fig. 1(a). In densely packed highly ordered structures a slipped arrangement is preferred, emphasizing the known tendency of the central metal atoms of phthalocyanines to interact with the mesobridged nitrogen atoms of adjacent molecules [38].

The molecules on top of the first SnPc BL mostly grow as further BLs with Sn-up and Sn-down configurations in odd- and even-numbered layers, respectively. In Fig. 1(d) an STM image of the fourth layer is shown consisting of only Sn-down molecules. A Sn-up molecule as a representative of the third layer is marked by a white dashed circle. This molecule is slipped by about half of the length of the longer unit-cell vector with respect to the corresponding Sn-down molecule in the top layer, which mimics the structure suggested for the SnPc BL. Further, the surface unit cell is superimposed on the image whose parameters have been obtained from the LEED measurement in Fig. 1(f). The surface unit cell and the orientation of the molecules are thereby almost identical to the first BL; only the second unit-cell vector is now ≈ 0.2 Å shorter, but this may be insignificant with respect to the higher experimental uncertainty (0.4 Å).

B. Optical spectroscopy

SnPc thin films were characterized by means of *in situ* DRS, which probes the optical absorption behavior of the film. The discussion is based on the imaginary part of the dielectric function shown in Fig. 4, which has been numerically extracted (see Experimental Details section) from the DRS raw data shown in Fig. 3 of the Supplemental Material. To this end the DRS baseline was set after preparing the PTCDA ML on Ag(111). The film thickness d^* given in the graph thus corresponds to the effective film thickness of only the SnPc adlayer.

1. SnPc monolayer

The spectrum of the first SnPc ML consists of a main peak at 1.71 eV followed by a small shoulder at approximately 1.86 eV. This signature has already been discussed in a previous publication [19]. Briefly, the optical signature in the first ML can be clearly assigned to the Q band of SnPc monomers, as observed in benzene or on inert mica [see Fig. 4(c)]. The occurrence of monomers is a consequence of the PTCDA interlayer serving as a decoupling layer for SnPc molecules, meaning that no noticeable electronic interaction takes place across the hetero-organic interface and, especially, no significant coupling to metal substrate states can be found. The optical absorption behavior can principally be understood qualitatively by the Kasha model [16], albeit simplified since transition dipoles are treated as pointlike. In this framework the appearance of optical spectra depends on the relative orientation of transition dipole moments and the distance of centers of gravity of the molecules. In the case of phthalocyanines two transition dipole moments need to be taken into account for symmetry reasons. Both are parallel to the molecular plane, and they are orthogonal to each other. Further, the corresponding transitions are energetically degenerate for isolated molecules [39], which is nearly the case for SnPc up

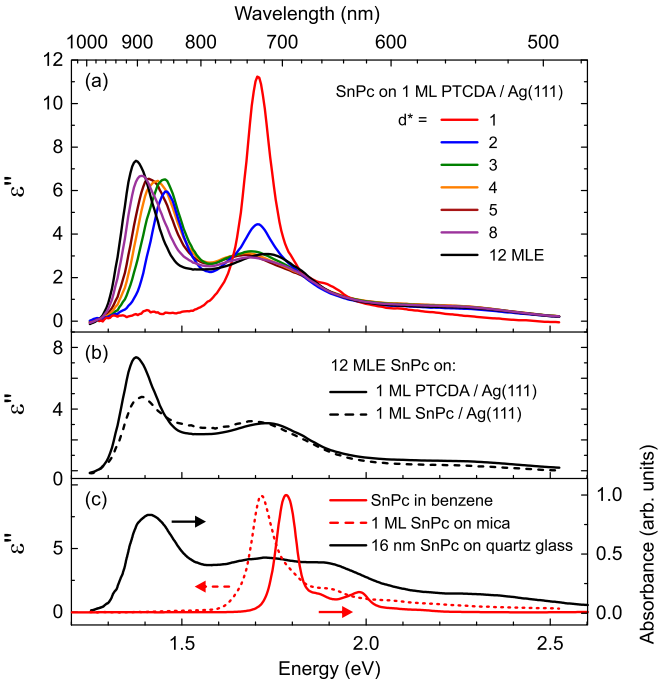

FIG. 4. (a) Imaginary part of the dielectric function ε'' of SnPc on 1 ML PTCDA/Ag(111), numerically extracted from the DRS data in Fig. 3 in the Supplemental Material. (b) ε'' spectrum of 12 MLE SnPc on 1 ML SnPc/Ag(111) [22] shown for comparison. (c) Normalized absorbance spectra of SnPc in benzene, 16 nm SnPc on quartz glass [40], and ε'' spectrum of SnPc on inert mica [22] for comparison. The arrows point to the ordinate corresponding to the respective curves. The small energetic shifts between the measurements on mica and in benzene may be explained by the different polarizabilities (dielectric backgrounds), while the 1 ML film on mica may additionally be affected by two-dimensional molecular aggregation [41], which is absent in solution.

to 1 ML. Coupling to neighboring molecules is quite small due to very weak spatial and/or energetic overlap of the orbitals of SnPc and PTCDA on the one hand and the relatively large distance of approximately 1.3 nm between the centers of gravity of SnPc within the monolayer on the other hand.

2. SnPc bilayer

Upon formation of stacked SnPc molecules an increased orbital overlap can give rise to an energetic separation and/or shifts of the optical transition energies. In fact, the ε'' spectrum changes abruptly from the second ML on (see Fig. 4). Then the vertical distance between stacked SnPc molecules is only approximately 0.34 nm [34,35], resulting in noticeable overlap of π orbitals which extend out of plane while the in-plane orbital overlap still remains quite weak. This process can be regarded as a formation of quasi-one-dimensional physical aggregates extending in the stacking direction [see Fig. 3(b)]. Their sizes scale thereby with the number of molecules being stacked. In the case of the bilayer, the monomer signal disappears in favor of the dimer spectrum with prominent peaks at 1.46 and 1.71 eV.

It has been shown that the two main absorption bands of phthalocyanine dimers can basically be understood in the

framework of an excitonic theory [42]. The strong redshift of the absorption indicates that the transition dipole moments of the molecules being coupled are essentially arranged head to tail, having thus J-aggregate character. This is in agreement with our structural suggestion for the dimers in Fig. 3, where the two molecules of each dimer are presumably in a slipped cofacial geometry. Moreover, the energetic positions of the two main absorption bands depend on the relative slipping distance [42]. However, understanding the optical absorption in detail is more complex. A splitting of the highest occupied molecular orbital (HOMO) has been experimentally observed for the SnPc BL on 1 ML PTCDA/Ag(111) [24]. For PbPc on highly oriented pyrolytic graphite it has been explicitly shown that HOMO splitting originates from $\pi-\pi$ interactions between vertically stacked molecules of a BL [43]. Such a strong orbital overlap can principally manifest itself in the optical absorption behavior; for example, it is known that the molecular excitation can delocalize preferentially along directions where the strongest electronic dispersion occurs [44]. The optical properties might then be attributed to an admixture of Frenkel and charge-transfer excitons [45].

The electronic absorption spectra of SnPc monomers and aggregates have been calculated recently by time-dependent density functional theory (TD-DFT) [11]. Owing to the two-molecule unit cell of triclinic SnPc two different types of dimers, convex and concave, can be distinguished [11]. From our structural investigation we find that the SnPc BL on top of 1 ML PTCDA/Ag(111) most likely consists of convex-type dimers. The corresponding DFT calculations reveal a reduced HOMO-LUMO gap upon dimer formation of SnPc [11]. Further, the low-energy absorption peak mainly stems from HOMO to lowest unoccupied molecular orbital (LUMO) and to LUMO+1 transitions [11]. Consequently, the strong redshift of the absorption can be mainly attributed to a relatively strong $\pi-\pi$ interaction. The peaks in the Q-band region additionally contain large contributions from the central metal atom.

3. *Stacked bilayers*

Our STM data indicate that additional molecules on top of the first BL arrange themselves in further BLs, which is in agreement with structural investigations on similar films [43,46]. The film thicknesses beyond the first BL are thus given as monolayer equivalents (MLE; 1 BL = 2 MLE) in the following. The optical spectra of 3 and 4 MLE are thus representative of the growth of the second SnPc BL.

Basically, the spectrum of the 3 MLE film is very similar to that of the SnPc dimers. The low-energy transition band is slightly redshifted by only ≈ 6 meV, and the former Q-band region at around 1.7 eV is additionally broadened. Bearing in mind the strong redshift upon formation of the first BL, orbital overlap between consecutive BLs must therefore be considerably weaker. In fact, the formation of *extended* electronic bands in case of PbPc multilayers has been excluded from results obtained with photoelectron spectroscopy [43].

The main difference between the 3 and 4 MLE films is the filling factor of the second BL. This means that the spectral changes of the ε'' spectra from 3 to 4 MLE should basically be identical to the changes from 2 to 3 MLE. However, for the fourth MLE film an even more redshifted component evolves. This clearly points to the beginning formation of further BLs prior to completion of the second BL.

By further increasing the film thickness the aggregates become even larger. Thus their optical fingerprint converges towards a bulk spectrum represented by the 12 MLE film in Fig. 4(a). The corresponding ε'' spectrum can be primarily attributed to large quasi-one-dimensional aggregates which account for an intense absorption band at 1.37 eV. A similar spectral appearance has already been observed for SnPc and other shuttlecock-type phthalocyanines in triclinic polymorphs [10–13]. The full width at half maximum (FWHM) of the low-energy transition band for the 12 MLE film is particularly small, which is characteristic for large J aggregates. As reasoned in the literature, this is a consequence of coherently coupled transition dipole moments of molecules in extended J-type arrangements [18]. It is thus plausible that finite domain sizes, defects, and disorder would limit the number of molecules in such stacks with the tendency of a less pronounced redshift and stronger spectral broadening.

The impact of structural ordering on the optical fingerprint shall be demonstrated for a comparable film where the PTCDA interlayer is replaced by a SnPc monolayer. The SnPc layer in contact with Ag(111) fulfills, in analogy to the PTCDA interlayer, a decoupling function in terms of electronic interaction [22,25]. Consequently, a SnPc monolayer on top of the decoupling layer shows essentially monomeric behavior in both cases. Multilayers of SnPc with a SnPc instead of a PTCDA interlayer, however, are characterized by broadened absorption features that are less intense in the NIR. The low-energy peak of a SnPc multilayer film has its maximum at 1.39 eV and is significantly broader than the film where the PTCDA interlayer is used [see Fig. 4(b)]. In fact, the optical absorption is very similar to that of a polycrystalline film on quartz glass [see Fig. 4(c)]. The main difference is that the pure SnPc multilayer film on Ag(111) consists of a mixture of different phases, each with dissimilar unit-cell geometries and molecular orientations [46]. We were not able to obtain sharp diffraction spots in LEED for a 10 MLE SnPc film on Ag(111) under similar preparation conditions as applied here using the PTCDA/Ag(111) substrate. The polycrystallinity is therefore responsible for an effective broadening of the spectra of a SnPc multilayer film directly on Ag(111) because (i) each distinct phase gives rise to aggregates with dissimilar contributions to the optical absorption spectrum and (ii) the number of transition dipole moments being coherently coupled is rather limited due to small quasi-one-dimensional aggregates. In contrast, the significantly narrower low-energy transition of SnPc multilayer films grown on the PTCDA interlayer is readily explainable as a consequence of the strongly improved structural ordering in this case, where sharp diffraction spots can be observed even for more than 10 MLEs of SnPc (see Fig. 4 in the Supplemental Material).

C. Conclusion

We have investigated the structures of SnPc layers on top of 1 ML PTCDA/Ag(111). We found that the SnPc monolayer is entirely rearranged upon BL formation. The corresponding structure is commensurate in higher order with respect to the PTCDA monolayer. The role of the latter is that of a

buffer layer preventing the SnPc molecules from interacting directly with the metal substrate states. Further, the PTCDA layer modifies the surface potential landscape of Ag(111), e.g., lowering the intrinsic symmetry of the surface by the PTCDA herringbone arrangement. Consequently, the SnPc BL forms only one structure with no additional rotational or mirror domains than those already encountered for PTCDA. The BL consists of SnPc dimers providing a characteristic absorption spectrum with strongly redshifted components compared to the monomer absorption. We elucidated that this shift mainly stems from a relatively strong orbital overlap between the molecules of each dimer. Intriguingly, the first BL of SnPc closely resembles the absorption characteristics of a multilayer film. Although the molecules in additional BLs on top adopt very similar structures, the optical absorption of the film is affected only to a minor extent. Consequently, the SnPc multilayer film can be regarded as a stack of BLs with weak orbital overlap between adjacent BLs. Each BL thereby contributes a similar dimer signature to the absorption spectrum. The additional redshift of the low-energy transition band with increasing film thickness can be attributed to inter-BL interaction, which has the character of transition dipole coupling with the molecules in a J-type arrangement. We demonstrated that this effect is much more pronounced when high structural ordering of the SnPc film is achieved.

ACKNOWLEDGMENTS

This work was financed by the Deutsche Forschungsgemeinschaft (DFG) through Grants No. FR875/9-3 and No. INST 275/256-1 FUGG. We thank Dr. A. Schöll and Dr. C. Sauer for providing the SnPc. Further, we thank Prof. Dr. C. Ronning for making the *ex situ* UV-VIS spectrometer available to us.

[1] S. Liu, W. M. Wang, A. L. Briseno, S. C. B. Mannsfeld, and Z. Bao, Adv. Mater. **21**, 1217 (2009).
[2] S. Reineke, M. Thomschke, B. Lüssem, and K. Leo, Rev. Mod. Phys. **85**, 1245 (2013).
[3] K. Walzer, B. Maennig, M. Pfeiffer, and K. Leo, Chem. Rev. **107**, 1233 (2007).
[4] F. Zhu, M. Grobosch, U. Treske, L. Huang, W. Chen, J. Yang, D. Yan, and M. Knupfer, ACS Appl. Mater. Interfaces **3**, 2195 (2011).
[5] C. Poelking, M. Tietze, C. Elschner, S. Olthof, D. Hertel, B. Baumeier, F. Würthner, K. Meerholz, K. Leo, and D. Andrienko, Nat. Mater. **14**, 434 (2015).
[6] F. Quochi, G. Schwabegger, C. Simbrunner, F. Floris, M. Saba, A. Mura, H. Sitter, and G. Bongiovanni, Adv. Optical Mater. **1**, 117 (2013).
[7] Z. Wang, T. Wang, H. Wang, and D. Yan, Adv. Mater. **26**, 4582 (2014).
[8] L. Huang, F. Zhu, C. Liu, U. Treske, M. Grobosch, H. Tian, J. Zhang, Y. Geng, M. Knupfer, and D. Yan, Adv. Funct. Mater. **22**, 4598 (2012).
[9] T. Breuer and G. Witte, ACS Appl. Mater. Interfaces **7**, 20485 (2015).
[10] M. Hiramoto, K. Kitada, K. Iketaki, and T. Kaji, Appl. Phys. Lett. **98**, 023302 (2011).
[11] M. Sumimoto, T. Honda, Y. Kawashima, K. Hori, and H. Fujimoto, RSC Adv. **2**, 12798 (2012).
[12] A. Yamashita, S. Matsumoto, S. Sakata, T. Hayashi, and H. Kanbara, J. Phys. Chem. B **102**, 5165 (1998).
[13] K. Walzer, T. Toccoli, A. Pallaoro, S. Iannotta, C. Wagner, T. Fritz, and K. Leo, Surf. Sci. **600**, 2064 (2006).
[14] L. Edwards and M. Gouterman, J. Mol. Spectrosc. **33**, 292 (1970).
[15] J. Mack and M. J. Stillman, Coord. Chem. Rev. **219–221**, 993 (2001).
[16] M. Kasha, H. R. Rawls, and M. Ashaf El-Bayoumi, Pure Appl. Chem. **11**, 371 (1965).
[17] F. C. Spano, Acc. Chem. Res. **43**, 429 (2010).
[18] F. Würthner, T. E. Kaiser, and C. R. Saha-Möller, Angew. Chem. Int. Ed. **50**, 3376 (2011).
[19] M. Gruenewald, C. Sauer, J. Peuker, M. Meissner, F. Sojka, A. Schöll, F. Reinert, R. Forker, and T. Fritz, Phys. Rev. B **91**, 155432 (2015).
[20] D. E. Hooks, T. Fritz, and M. D. Ward, Adv. Mater. **13**, 227 (2001).
[21] C. Wagner, R. Forker, and T. Fritz, J. Phys. Chem. Lett. **3**, 419 (2012).
[22] M. Gruenewald, K. Wachter, M. Meissner, M. Kozlik, R. Forker, and T. Fritz, Org. Electron. **14**, 2177 (2013).
[23] R. G. Musket, W. McLean, C. A. Colmenares, D. M. Makowiecki, and W. J. Siekhaus, Appl. Surf. Sci. **10**, 143 (1982).
[24] M. Häming, M. Greif, M. Wießner, A. Schöll, and F. Reinert, Surf. Sci. **604**, 1619 (2010).
[25] M. Häming, M. Greif, C. Sauer, A. Schöll, and F. Reinert, Phys. Rev. B **82**, 235432 (2010).
[26] B. Stadtmüller, T. Sueyoshi, G. Kichin, I. Kröger, S. Soubatch, R. Temirov, F. S. Tautz, and C. Kumpf, Phys. Rev. Lett. **108**, 106103 (2012).
[27] S. Torbrügge, O. Schaff, and J. Rychen, J. Vac. Sci. Technol. B **28**, C4E12 (2010).
[28] F. Sojka, M. Meissner, C. Zwick, R. Forker, and T. Fritz, Rev. Sci. Instrum. **84**, 015111 (2013).
[29] Scienta Omicron, LEEDLAB, version 1.64, http://www.scientaomicron.com/en/products/350/1155.
[30] R. Forker and T. Fritz, Phys. Chem. Chem. Phys. **11**, 2142 (2009).
[31] R. Forker, M. Gruenewald, and T. Fritz, Annu. Rep. Prog. Chem., Sect. C: Phys. Chem. **108**, 34 (2012).
[32] M. Möbus, N. Karl, and T. Kobayashi, J. Cryst. Growth **116**, 495 (1992).
[33] A. A. Levin, T. Leisegang, R. Forker, M. Koch, D. C. Meyer, and T. Fritz, Cryst. Res. Technol. **45**, 439 (2010).
[34] M. K. Friedel, B. F. Hoskins, R. L. Martin, and S. A. Mason, J. Chem. Soc. D 400 (1970).
[35] R. Kubiak and J. Janczak, J. Alloys Compd. **189**, 107 (1992).

[36] See Supplemental Material at http://link.aps.org/supplemental/10.1103/PhysRevB.93.115418 for STM image of domain boundaries of SnPc on 1 ML PTCDA/Ag(111) at a silver step; contrast-enhanced STM image of a SnPc BL on 1 ML PTCDA/Ag(111) revealing the commensurate supercell; measured DRS data used for the extraction of the dielectric function; and LEED image of a SnPc multilayer on 1 ML PTCDA/Ag(111).

[37] S. van Smaalen, *Incommensurate Crystallography*, IUCr Monographs on Crystallography (Oxford University Press, Oxford, 2007).

[38] L.-K. Chau, C. D. England, S. Chen, and N. R. Armstrong, J. Phys. Chem. **97**, 2699 (1993).

[39] J. D. Baran and J. A. Larsson, Phys. Chem. Chem. Phys. **12**, 6179 (2010).

[40] F. Yang, R. R. Lunt, and S. R. Forrest, Appl. Phys. Lett. **92**, 053310 (2008).

[41] M. Müller, E. Le Moal, R. Scholz, and M. Sokolowski, Phys. Rev. B **83**, 241203(R) (2011).

[42] Y. Sakakibara, K. Saito, and T. Tani, Jpn. J. Appl. Phys. **37**, 695 (1998).

[43] S. Kera, H. Fukagawa, T. Kataoka, S. Hosoumi, H. Yamane, and N. Ueno, Phys. Rev. B **75**, 121305(R) (2007).

[44] S. Sharifzadeh, C. Y. Wong, H. Wu, B. L. Cotts, L. Kronik, N. S. Ginsberg, and J. B. Neaton, Adv. Funct. Mater. **25**, 2038 (2015).

[45] V. Agranovich, K. Schmidt, and K. Leo, Chem. Phys. Lett. **325**, 308 (2000).

[46] Y. Wang, J. Kröger, R. Berndt, and W. Hofer, Angew. Chem. Int. Ed. **48**, 1261 (2009).